

A Time Splitting Based Optimization Method for Nonlinear MHE

Shuting Wu[†], Yifei Wang[†], Jingzhe Wang and Xu Du^{*}

Abstract—Moving Horizon Estimation (MHE) is essentially an optimization-based approach designed to estimate the states of dynamic systems within a moving time horizon. Traditional MHE solutions become computationally prohibitive due to the *curse of dimensionality* arising from increasing problem complexity and growing length of time horizon. To address this issue, we propose novel computationally efficient algorithms for solving nonlinear MHE problems. Specifically, we first introduce a distributed reformulation utilizing a time-splitting technique. Leveraging this reformulation, we develop the Efficient Gauss-Newton Augmented Lagrangian Alternating Direction Inexact Newton (ALADIN) to achieve computational efficiency. Additionally, to accommodate limited computational capabilities inherent in some sub-problem solvers, we propose the Efficient Sensitivity Assisted ALADIN, which enables sub-problems to be solved inexactly without hindering computational efficiency. Furthermore, recognizing scenarios where sub-problem solvers possess no computational power, we propose a Distributed Sequential Quadratic Programming (SQP) that relies solely on first- and second-order information of local objective functions. We demonstrate the performance and advantages of our proposed methods through numerical experiments on differential drive robots case, a practical nonlinear MHE problem. Our results demonstrate that the three proposed algorithms achieve computational efficiency while preserving high accuracy, thereby satisfying the real-time requirements of MHE.

I. INTRODUCTION

Moving Horizon Estimation (MHE) has attracted considerable interest for its applications in differential drive robots [14], unmanned aerial vehicles [23], and wireless communication [25]; a comprehensive overview is provided in [17]. Essentially, MHE is an optimization-based approach for estimating the states of dynamic systems within a moving time horizon, providing an effective framework for state estimation in nonlinear and constrained dynamic systems. Current MHE approaches mainly rely on centralized solvers, yet these methods become computationally prohibitive as estimation complexity and the length of time horizon increase - a challenge commonly described as the *curse of dimensionality*. To address this challenge, one promising approach is to

reformulate MHE as a distributed optimization problem and adopt parallel algorithms for its solution. However, to the best of our knowledge, a suitable algorithm that efficiently solves distributed MHE has not yet been identified.

A natural approach for solving the distributed optimization reformulation of MHE is to adopt Augmented Lagrangian Alternating Direction Inexact Newton (ALADIN) [11], a distributed non-convex optimization algorithm known for integrating the advantages of Alternating Direction Method of Multipliers (ADMM) [3], [13] and Distributed Sequential Quadratic Programming (SQP) [15]. This motivation arises from ALADIN's demonstrated success in efficiently addressing Model Predictive Control problem (MPC) [10], [18], [16], [20], [22]- an optimization counterpart of MHE. ALADIN exhibits global convergence for convex problems and local convergence for non-convex problems [9], [6], with [7] establishing a global convergence theory for ALADIN in the context of non-convex problems. Typically, ALADIN solves sub-problems using an appropriate nonlinear programming (NLP) solver and coordinates information by solving a coupled quadratic programming (QP) problem. However, directly applying standard ALADIN [8] to MHE remains computationally expensive due to the inherent coupled QP step required for coordinating distributed information, rendering it unsuitable for the real-time requirements of MHE. While a variant of ALADIN tailored for MPC [10] might be considered, it targets general objective functions rather than the specific least-squares objective of MHE. Although a variant of ALADIN, known as Gauss-Newton ALADIN [5], exists for handling least-squares objectives, it remains computationally inefficient due to the coupled QP step. Thus, this gap motivates the following research question: *Can we develop computationally efficient variants of ALADIN specifically tailored to nonlinear MHE?*

Our Contribution: In this paper, we introduce a novel time-splitting-based optimization framework for solving nonlinear MHE problems efficiently while maintaining accuracy. We first revisit the nonlinear MHE formulation and propose a time-splitting-based distributed reformulation, extending the temporal decomposition concept originally developed for MPC [10]. Our reformulation partitions the time horizon into multiple independent sub-windows, significantly reducing sub-problems dimensionality. Leveraging this distributed reformulation, we develop computationally efficient solutions within the ALADIN framework. Specifically, to eliminate the computational overhead associated with iterative QP solutions required in ALADIN, we first derive a closed-form solution for the QP step. Exploiting this closed-form solution, we propose Efficient Gauss-Newton ALADIN, an accelerated

* Corresponding author.

[†] The first two authors contributed equally to this work.

Shuting Wu is with School of Mathematics and Statistics, North China University of Water Resources and Electric Power, Zhengzhou, China. Shuting Wu is also with the HNAS Institute of Mathematics, Henan Academy of Science. E-mail: wushuting0126@163.com.

Yifei Wang is with the Ningbo Artificial Intelligence Institute and the Department of Automation, Shanghai Jiao Tong University, Shanghai 200240, China. E-mail: yifeiw4ng@sjtu.edu.cn.

Jingzhe Wang is with School of Computing and Information, University of Pittsburgh, Pittsburgh, PA, USA. E-mail: jiw148@pitt.edu.

Xu Du is with the Artificial Intelligence Thrust of the Information Hub, The Hong Kong University of Science and Technology (Guangzhou), Guangzhou, China. E-mail: duxu@hnas.ac.cn.

variant of Gauss-Newton ALADIN algorithm introduced in [5], which achieves computational efficiency. Additionally, considering practical scenarios where sub-problem solvers possess limited computational power, we introduce Efficient Sensitivity Assisted ALADIN, inspired by [12], which allows the sub-problems step to be solved inexactly. We further consider an extreme scenario wherein sub-problem solvers have no computational capability. Under this stringent condition, inspired by [21], we develop an Efficient Distributed SQP that entirely eliminates explicit sub-problem solving. Instead, it only evaluates first- and second-order information of local objectives.

To validate our methods, we conduct numerical benchmarks on the differential drive robots problem, a practical nonlinear MHE problem involving 3 states and 2 control inputs per time slot across a total horizon length of 25 time slots. The results demonstrate that our Efficient Distributed SQP achieves identical state estimation trajectories to those obtained by CasADi [14]. Moreover, all three proposed algorithms consistently achieve convergence precision of 10^{-8} within 30 iterations. Notably, the fastest algorithm among them requires only 0.02 seconds to reach 50 iterations.

Organization: The paper is structured as follows: In Section II, we provide key preliminaries for MHE. Section III details our proposed time-splitting-based reformulation of MHE. In Section IV, we provide our novel algorithms. Numerical evaluations are presented in Section V. Finally, Section VI concludes the paper.

II. FUNDAMENTALS OF THE MHE

A. Discrete Control System

In control systems, dynamic behavior is typically modeled using discrete-time nonlinear equations, comprising state and output equations that characterize system evolution and observation relationships at time index n ,

$$\begin{aligned} x_{n+1} &= f(x_n, u_n), \\ y_n &= h(x_n) + v_n. \end{aligned} \quad (1)$$

Here, $x_n \in \mathbb{R}^{|x_n|}$ denotes the system state, $u_n \in \mathbb{R}^{|u_n|}$ represents the control input, and $y_n \in \mathbb{R}^{|y_n|}$ stands for the measured output. Note that the measurement noise v_n follows a zero-mean Gaussian distribution, i.e., $v_n \sim \mathcal{N}(0, V)$, where V is a positive-definite covariance matrix. Furthermore, the nonlinear dynamics is defined by $f : \mathbb{R}^{|x_n|+|u_n|} \rightarrow \mathbb{R}^{|x_n|}$, and the nonlinear measurement function is expressed by $h : \mathbb{R}^{|x_n|} \rightarrow \mathbb{R}^{|y_n|}$, both of which are assumed to be twice continuously differentiable.

B. Basics of MHE

Based on (1), at each time step l , given a prediction horizon of length L , the following optimization problem represents a formulation of MHE (see [14]),

$$\begin{aligned} \min_{x, u} \quad & \frac{1}{2} \|x_{l-L} - \hat{x}_{l-L}\|_{P^{-1}}^2 + \frac{1}{2} \sum_{n=l-L}^l \|h(x_n) - y_n\|_{V^{-1}}^2 \\ & + \frac{1}{2} \sum_{n=l-L}^{l-1} \|u_n - \hat{u}_n\|_{W^{-1}}^2 + \frac{1}{2} \sum_{n=l-L}^{l-1} \|x_{n+1} - f(x_n, u_n)\|_{R^{-1}}^2. \end{aligned} \quad (2)$$

The optimization variable is defined as,

$$\begin{cases} x = (x_{l-L}^\top, x_{l-L+1}^\top, \dots, x_l^\top)^\top, \\ u = (u_{l-L}^\top, u_{l-L+1}^\top, \dots, u_{l-1}^\top)^\top, \end{cases} \quad (3)$$

where \hat{x}_{l-L} represents the prior state estimate, $P \in \mathbb{R}^{|x_n| \times |x_n|}$ denotes the covariance matrix associated with the initial state estimation error, $R \in \mathbb{R}^{|x_n| \times |x_n|}$ corresponds to the covariance matrix of the state noise, $V \in \mathbb{R}^{|y_n| \times |y_n|}$ describes the covariance matrix of the observation noise, and $W \in \mathbb{R}^{|u_n| \times |u_n|}$ characterizes the covariance matrix of the control input variations. In this expression, the optimization variables of Problem (2) are x and u .

An alternative MHE formulation considers only x as the optimization variable. Although u still appears in the expressions, it is treated as a known constant. Based on this, the simplified optimization problem is formulated as follows¹ (see [24]):

$$\begin{aligned} \min_x \quad & \frac{1}{2} \|x_{l-L} - \hat{x}_{l-L}\|_{P^{-1}}^2 + \frac{1}{2} \sum_{n=l-L}^l \|h(x_n) - y_n\|_{V^{-1}}^2 \\ \text{s.t.} \quad & x_{n+1} = f(x_n, u_n), \quad \forall n = l-L, \dots, l-1. \end{aligned} \quad (4)$$

This paper focuses on the MHE optimization problem formulated in (4).

III. DISTRIBUTED MHE REFORMULATION: A TIME-SPLITTING-BASED APPROACH

This section introduces a time-splitting-based distributed MHE framework built on (4). By partitioning the time horizon into multiple independent sub-windows, this approach significantly reduces the dimensionality of the sub-problems.

A. Components of the Time Splitting Reformulation

To mitigate computational complexity and enhance real-time performance in Problem (4), the time window $[l-L, l]$ is divided into N consecutive sub-windows. The first $(N-1)$ sub-windows each have a length of $t = \lfloor \frac{L}{N} \rfloor$, while the last sub-window has a length of $t_N = L - (N-1)t$, where $N, t, t_N \in \mathbb{N}_{>0}$. Accordingly, the time range for the i -th sub-window is given by $[l-L + (i-1)t, l-L + it]$, ($i = 1, 2, \dots, N-1$). For the last sub-window ($i = N$), the time range is $[l-L + (N-1)t, l]$. Importantly, the auxiliary variable $z = ((z_1)^\top, (z_2)^\top, \dots, (z_N)^\top)^\top$ is introduced to represent the *boundary state* of each sub-window. Here, $z_i = ((z_i^a)^\top, (z_i^b)^\top)^\top$ with z_i^a denoting the *initial state* of the i -th sub-window, defined as $z_i^a = x_{l-L+(i-1)t}$. In subsequent sections, $x_{l-L+(i-1)t}$ will be replaced by z_i^a . Meanwhile, z_i^b serves as a new auxiliary variable representing the *terminal state* of the i -th sub-window.

The optimization variable X_i associated with the local optimization problem for the i -th sub-window is defined as:

$$X_i = ((z_i^a)^\top, (\tilde{x}_{(i)})^\top, (z_i^b)^\top)^\top, \quad X_i \in \mathbb{R}^{|X_i|},$$

¹For the convenience of the subsequent expressions, this paper studies MHE without inequality constraints. See [2], [4], [19] for a similar setting.

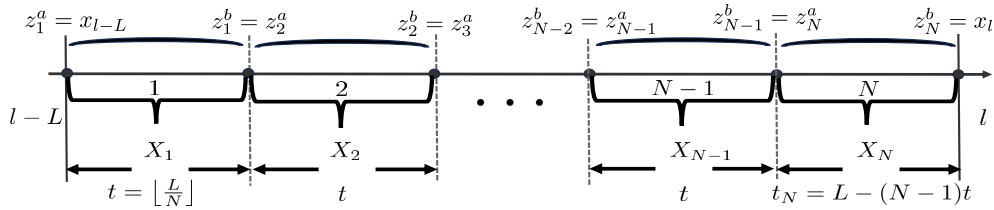


Fig. 1: The time-splitting-based MHE

where $\tilde{x}^{(i)}$ represents the *internal states* of the i -th sub-window, such that $\tilde{x}^{(i)} \in \mathbb{R}^{|\tilde{x}^{(i)}|}$, and is expressed as:

$$\tilde{x}^{(i)} = \begin{cases} ((x_{l-L+(i-1)t+1})^\top, \dots, (x_{l-L+it-1})^\top)^\top, & i=1, \dots, N-1, \\ ((x_{l-L+(N-1)t+1})^\top, \dots, (x_{l-1})^\top)^\top, & i=N. \end{cases}$$

Here, $|X_i| = |z_i^a| + |\tilde{x}^{(i)}| + |z_i^b|$.

With the above definitions, a schematic diagram of the *time-splitting-based MHE*, where $z_i^b = z_{i+1}^a$ is illustrated in Figure 1. Further details are provided in Section III-B.

The objective function for each sub-problem is represented by $J_i(X_i) : \mathbb{R}^{|X_i|} \rightarrow \mathbb{R}$, and the optimization problem for the i -th sub-window is formulated as follows, for $i = 1$ and $i = N$,

$$\begin{cases} J_1(X_1) = \frac{1}{2} \|z_1^a - \hat{x}_{l-L}\|_{P-1}^2 + \frac{1}{2} \sum_{j=l-L}^{l-L+t-1} \|h(x_j) - y_j\|_{V-1}^2, \\ J_N(X_N) = \frac{1}{2} \sum_{j=l-L+(N-1)t}^l \|h(x_j) - y_j\|_{V-1}^2, \end{cases} \quad (5)$$

for $i = 2, \dots, N-1$,

$$J_i(X_i) = \frac{1}{2} \sum_{j=l-L+(i-1)t}^{l-L+it-1} \|h(x_j) - y_j\|_{V-1}^2. \quad (6)$$

Analogous to the objective function formulation, the nonlinear dynamic equality constraints are partitioned into sub-vectors independently as follows, for $i = 1, \dots, N-1$,

$$\mathcal{F}_i(X_i) = \begin{bmatrix} x_{l-L+(i-1)t+1} - f(z_i^a, u_{l-L+(i-1)t}) \\ x_{l-L+(i-1)t+2} - f(x_{l-L+(i-1)t+1}, u_{l-L+(i-1)t+1}) \\ \vdots \\ z_i^b - f(x_{l-L+it-1}, u_{l-L+it-1}) \end{bmatrix}, \quad (7)$$

for $i = N$:

$$\mathcal{F}_i(X_i) = \begin{bmatrix} x_{l-L+(i-1)t+1} - f(z_i^a, u_{l-L+(i-1)t}) \\ x_{l-L+(i-1)t+2} - f(x_{l-L+(i-1)t+1}, u_{l-L+(i-1)t+1}) \\ \vdots \\ x_l - f(x_{l-1}, u_{l-1}) \end{bmatrix}. \quad (8)$$

B. The Time Splitting Reformulation of MHE

Consequently, based on (5)-(8), the time-splitting-based formulation of MHE can be represented as:

$$\begin{aligned} \min_{\{X_i\}} \quad & \sum_{i=1}^N J_i(X_i) \\ \text{s.t.} \quad & \mathcal{F}_i(X_i) = 0 \quad |\mu_i, \quad \forall i = 1, \dots, N, \\ & \sum_{i=1}^N A_i X_i = 0 \quad |\lambda. \end{aligned} \quad (9)$$

Here, μ_i represents the dual variable of the sub-constraint \mathcal{F}_i , where its dimension is given by,

$$|\mu_i| = \begin{cases} |X_i|(t-1), & i = 1, 2, \dots, N-1, \\ |X_i|(t_N-1), & i = N, \end{cases}$$

while $\lambda \in \mathbb{R}^{(N-1)|z_1^b|}$ denotes the Lagrange multiplier corresponding to the coupling constraints. The coupling constraint matrix A_i is structurally defined as follows,

$$\begin{aligned} A_1 &= \begin{bmatrix} \bar{\mathbf{0}} & \hat{\mathbf{0}} & I_{|z_1^b|} \\ \bar{\mathbf{0}} & \hat{\mathbf{0}} & \mathbf{0} \\ \vdots & \vdots & \vdots \end{bmatrix}, \quad A_N = \begin{bmatrix} \vdots & \vdots & \vdots \\ \bar{\mathbf{0}} & \mathbf{0}^{(N)} & \bar{\mathbf{0}} \\ -I_{|z_N^a|} & \mathbf{0}^{(N)} & \bar{\mathbf{0}} \end{bmatrix}, \\ \tilde{A} &= \begin{bmatrix} -I_{|z_i^a|} & \hat{\mathbf{0}} & \bar{\mathbf{0}} \\ \mathbf{0} & \hat{\mathbf{0}} & I_{|z_i^b|} \end{bmatrix}, \quad \forall i \in \{2, \dots, N-1\}, \\ A_i &= \begin{bmatrix} \mathbf{0}_{|X_i| \times (i-2)|z_1^b|}, & \tilde{A}^\top, & \mathbf{0}_{|X_i| \times (r-i)|z_1^b|} \end{bmatrix}^\top, \end{aligned}$$

where, matrix $\bar{\mathbf{0}} = \mathbf{0}_{|z_1^b| \times |z_1^b|}$; $\hat{\mathbf{0}} = \mathbf{0}_{|z_1^b| \times |\tilde{x}^{(1)}|}$; $\mathbf{0}^{(N)} = \mathbf{0}_{|z_1^b| \times |\tilde{x}^{(N)}|}$; such that $A_1 \in \mathbb{R}^{r \times |X_1|}$, $A_i \in \mathbb{R}^{r \times |X_i|}$, $A_N \in \mathbb{R}^{r \times |X_N|}$, $\tilde{A} \in \mathbb{R}^{2|z_i^b| \times |X_i|}$. Note that $\sum_{i=1}^N A_i X_i = 0$ contains $z_i^b = z_{i+1}^a$, for $i = 1, \dots, N-1$.

IV. DISTRIBUTED OPTIMIZATION ALGORITHMS

This section is dedicated to developing efficient solutions within the ALADIN framework to address the time-splitting reformulation of MHE (9). First, an efficient approach for solving coupled QP, which is integrated into the ALADIN framework, is proposed. Subsequently, based on the aforementioned efficient approach, three ALADIN variants are proposed to reduce the computational burden. In this section, $(\cdot)^+$ denotes the value after the update, whereas $(\cdot)^-$ represents the value before the update.

A. An Efficient Method for Solving Coupled QP

Before introducing our algorithm for solving Problem (9), we first introduce an efficient method for solving the strongly convex coupled QP (10).

$$\begin{aligned} \min_{\{\Delta X_i\}} \quad & \sum_{i=1}^N \frac{1}{2} \Delta X_i^\top H_i \Delta X_i + g_i^\top \Delta X_i \\ \text{s.t.} \quad & C_i \Delta X_i = 0 \quad |\mu_i, \quad \forall i = 1, \dots, N, \\ & \sum_{i=1}^N A_i (X_i^+ + \Delta X_i) = 0 \quad |\lambda. \end{aligned} \quad (10)$$

Theorem 1 (Efficient QP) *Let the linear independence constraint qualification (LICQ) be satisfied for Problem (10), ensuring the linear independence of C_i s and A_i s. Let the*

second-order sufficient condition (SOSC) [15] be satisfied, i.e., $H_i \succ 0, \forall i$. Assume the existence of a unique global optimal solution for Problem (10). Solving Problem (10) is equivalent to evaluating the values of λ , μ_i and ΔX_i as follows,

$$\begin{cases} \lambda = \left(\sum_{i=1}^N G_i - Q_i R_i^{-1} Q_i^\top \right)^{-1} p, \\ \mu_i = -R_i^{-1} \left(C_i H_i^{-1} g_i + Q_i^\top \lambda \right), \\ \Delta X_i = -H_i^{-1} \left(g_i + C_i^\top \mu_i + A_i^\top \lambda \right), \end{cases} \quad (11)$$

where,

$$\begin{cases} G_i = A_i H_i^{-1} A_i^\top, \\ Q_i = A_i H_i^{-1} C_i^\top, \\ R_i = C_i H_i^{-1} C_i^\top, \end{cases} \quad \begin{cases} q = \sum_{i=1}^N (Q_i R_i^{-1} C_i - A_i) H_i^{-1} g_i, \\ p = \sum_{i=1}^N A_i X_i^+ + q. \end{cases} \quad (12)$$

Proof. See Appendix I. \blacksquare

As an extension of Theorem 1, we propose the closed-form solution

$$\begin{cases} \lambda = \left(\sum_{i=1}^N G_i - Q_i R_i^{-1} Q_i^\top \right)^{-1} \left(p - \sum_{i=1}^N Q_i R_i^{-1} D_i \right), \\ \mu_i = -R_i^{-1} \left(C_i H_i^{-1} g_i + Q_i^\top \lambda - D_i \right), \\ \Delta X_i = -H_i^{-1} \left(g_i + C_i^\top \mu_i + A_i^\top \lambda \right). \end{cases} \quad (13)$$

of the following problem,

$$\begin{aligned} \min_{\{\Delta X_i\}} \quad & \sum_{i=1}^N \frac{1}{2} \Delta X_i^\top H_i \Delta X_i + g_i^\top \Delta X_i \\ \text{s.t.} \quad & D_i + C_i \Delta X_i = 0 \quad |\mu_i, \quad \forall i = 1, \dots, N, \\ & \sum_{i=1}^N A_i (X_i^+ + \Delta X_i) = 0 \quad |\lambda. \end{aligned} \quad (14)$$

Note that, Equation (11) and (13) will be integrated into our proposed algorithms. Due to space limitations, details are omitted here.

B. Algorithm Development

Based on [5], Section IV-B.1 introduces an efficient variant of Gauss-Newton ALADIN. Section IV-B.2 presents an inexact update version of ALADIN, inspired by [12]. Finally, Section IV-B.3, drawing inspiration from [21], explores an ALADIN variant in which sub-problems are not locally optimized.

1) **Efficient Gauss-Newton ALADIN:** The objective function $J_i(X_i)$ in Problem (9) is formulated as a nonlinear least-squares optimization problem, where the full vector-valued measurement function $\mathcal{H}_i(X_i)$ is introduced:

$$\mathcal{H}_i(X_i) = \begin{pmatrix} P^{-\frac{1}{2}} (z_1^a - \hat{x}_{l-L})_{i=1} \\ V^{-\frac{1}{2}} (h(x_j) - y_j)_{j \in \mathcal{I}_i} \\ V^{-\frac{1}{2}} (h(x_i) - y_i)_{i=N} \end{pmatrix}, \quad (15)$$

where, $\mathcal{I}_i = \{l-L+(i-1)t, \dots, l-L+it-1\}$. Consequently, the objective function $J_i(X_i)$ of the sub-problems can be expressed as $J_i(X_i) = \frac{1}{2} \|\mathcal{H}_i(X_i)\|^2$.

Efficient Gauss-Newton ALADIN is presented in Algorithm 1. Similar to Gauss-Newton ALADIN [5], it alternates

Algorithm 1 Efficient Gauss-Newton ALADIN

Initialization: Initial guess of dual variable λ and primal variables $\{Y_i\}$, $\forall i$, choose $\rho > 0$.

Output: Optimal solution $\{Y_i^*\}$.

Repeat:

1) Paralleled solve local NLP:

$$X_i^+ = \arg \min_{X_i} \frac{1}{2} \|\mathcal{H}_i(X_i)\|^2 + \lambda^\top A_i X_i + \frac{\rho}{2} \|X_i - Y_i^-\|^2 \quad (16)$$

s.t. $\mathcal{F}_i(X_i) = 0$.

2) Evaluate local variables and sensitivity matrix from X_i^+ :

$$\begin{cases} b_i = \mathcal{H}_i(X_i^+), \\ B_i = \nabla \mathcal{H}_i(X_i^+)^\top, \\ C_i = \nabla \mathcal{F}_i(X_i^+). \end{cases} \quad (17)$$

3) Assemble gradient and Hessian:

$$g_i = B_i b_i, \quad H_i = B_i B_i^\top. \quad (18)$$

4) Update and broadcast the global dual variable λ :

$$\lambda = \left(\sum_{i=1}^N G_i - Q_i R_i^{-1} Q_i^\top \right)^{-1} p. \quad (19)$$

5) Paralleled update local primal and dual variables:

$$\begin{cases} \mu_i = -R_i^{-1} (C_i H_i^{-1} g_i + Q_i^\top \lambda), \\ Y_i^+ = X_i^+ - H_i^{-1} (g_i + C_i^\top \mu_i + A_i^\top \lambda). \end{cases} \quad (20)$$

between solving sub-problems in parallel at the sub-nodes and coordinating via the coupled QP (10). Further, Algorithm 1 replaces the coupled QP with (11), thereby accelerating computation. During each iteration, Step 1) solves the NLP sub-problems (16) in parallel using any NLP solver. In Step 2), each sub-node performs sensitivity analysis based on its local solution, computing the gradient g_i and H_i at each local node according to the optimal solution X_i^+ , see (17). These results are then transmitted to the central node. After gathering the sensitivity data from all sub-nodes, the central node updates the global dual variable λ in Step 4) using Equation (19). The updated λ is subsequently broadcast to the sub-nodes, allowing each sub-node to locally update the primal variables according to Equation (20). This process is repeated until convergence.

Note that Algorithm 1 is specifically tailored for least-squares problems. To extend its applicability and further reduce overall computational time, we propose two additional ALADIN variants designed for broader problem classes.

2) **Efficient Sensitivity Assisted ALADIN:** Inspired by [12], we propose Efficient Sensitivity Assisted ALADIN (Algorithm 2) by leveraging the sensitivity of NLP parameters.

The augmented Lagrangian function for each sub-problem of Problem (9) is expressed as

$$\mathcal{L}_i = J_i(X_i) + \lambda^\top A_i (X_i - Y_i) + \frac{\rho}{2} \|X_i - Y_i\|^2 + \mu_i^\top \mathcal{F}_i(X_i). \quad (21)$$

Following the notation in [12, IV.C], we define $s_i(\xi_i) = (X_i(\xi_i)^\top, \mu_i(\xi_i)^\top)^\top$ for notational convenience, where $\xi_i = (Y_i^\top, \lambda^\top)^\top$. The Karush-Kuhn-Tucker (KKT) conditions for

the constrained sub-problems can be further expressed as,

$$\varphi_i(s_i(\xi_i^-), \xi_i^-) = \begin{bmatrix} \nabla_{X_i} \mathcal{L}_i(s_i(\xi_i^-)) \\ \mathcal{F}_i(X_i^-) \end{bmatrix} = 0, \quad (22)$$

where higher-order terms in the linearization of the solution manifold are neglected, the update for the sub-problems of Algorithm 2 is as follows,

$$s_i^+(\xi_i) = s_i(\xi_i^-) - \mathcal{M}_i^{-1} \mathcal{N}_i(\xi_i - \xi_i^-), \quad (23)$$

where $\mathcal{M}_i = \frac{\partial \varphi_i}{\partial s_i}$, $\mathcal{N}_i = \frac{\partial \varphi_i}{\partial \xi_i}$. Details can be found in [12, IV.C] and Appendix II. Utilizing a tangent predictor, the approximate solutions of the sub-problems at subsequent iterations can be efficiently estimated. Unlike the linearized ALADIN method [7, Equation (12), Appendix A], which linearizes the objective function around the current iteration point, this approach instead focuses on linearizing the solution manifold in the vicinity of the parameters.

Algorithm 2 Efficient Sensitivity Assisted ALADIN

Initialization: Initial guess of dual variable λ , μ_i , primal variables $\{Y_i = X_i\}$, $\forall i$ and parameter $\xi_0 = ((Y_i)^\top, \lambda^\top)^\top$, choose $\rho > 0$.

Output: Optimal solution $\{Y_i^*\}$.

Repeat:

- 1) Evaluate gradient, Hessian and sensitivity matrix from X_i :

$$\begin{cases} g_i = \nabla J_i(X_i), \\ H_i \approx \nabla^2 (J_i(X_i) + \mu_i^\top \mathcal{F}_i(X_i)) + \rho I, \\ C_i = \nabla \mathcal{F}_i(X_i), \\ D_i = \mathcal{F}_i(X_i). \end{cases} \quad (24)$$

- 2) Update and the global dual variable λ as

$$\lambda = \left(\sum_{i=1}^N G_i - Q_i R_i^{-1} Q_i^\top \right)^{-1} \left(p - \sum_{i=1}^N Q_i R_i^{-1} D_i \right). \quad (25)$$

- 3) Paralleled update μ_i s and Y_i^+ s as

$$\begin{cases} \hat{\mu}_i = -R_i^{-1} (C_i H_i^{-1} g_i + Q_i^\top \lambda - D_i), \\ Y_i^+ = X_i - H_i^{-1} (g_i + C_i^\top \hat{\mu}_i + A_i^\top \lambda). \end{cases} \quad (26)$$

- 4) Collect parameter $\xi_i = ((Y_i^+)^\top, \lambda^\top)^\top$, compute $\mathcal{M}_i, \mathcal{N}_i$ in parallel, and then solve local NLP with (23)².
 - 5) Extract X_i^+ from s_i^+ : $s_i^+ = ((X_i^+)^\top, \mu_i^\top)^\top$.
-

In Algorithm 2, inspired by (13), the central node updates the global dual variable according to Equation (25), incorporating local information from Equation (24). Each node then concurrently updates its local dual variable $\hat{\mu}_i$ and primal variable Y_i^+ via Equation (26). Next, each node updates s_i^+ using (23). This process iterates until convergence.

3) **Efficient Distributed SQP:** Building on the approach proposed in Decentralized SQP [21], we propose Efficient Distributed SQP (Algorithm 3). Unlike Algorithm 1 and 2, Algorithm 3 solves Problem (9) by bypassing the resolution of sub-problems. Moreover, instead of solving the coupled QP (14) via an inner-level ADMM [21], Algorithm 3 updates the global dual variable λ , the local variables μ_i and ΔX_i according to the closed-form given by (13).

²The update of local primal variables can optionally consist of two phases [12, Algorithm 1]: update using (23) when the KKT condition is almost satisfied; otherwise, update using (16).

Algorithm 3 Efficient Distributed SQP

Initialization: Initial guess of dual variable λ and primal variables $\{Y_i\}$, $\forall i$, choose $\rho > 0$.

Output: Optimal solution $\{Y_i^*\}$.

Repeat:

- 1) Locally update gradient, Hessian and sensitivity matrix from Y_i^- :

$$\begin{cases} g_i = \nabla J_i(Y_i^-), \\ H_i \approx \nabla^2 (J_i(Y_i^-) + \mu_i^\top \mathcal{F}_i(Y_i^-)) + \rho I, \\ C_i = \nabla \mathcal{F}_i(Y_i^-), \\ D_i = \mathcal{F}_i(Y_i^-). \end{cases} \quad (27)$$

- 2) Update and the global dual as Equation (25).

- 3) Update μ_i s and Y_i^+ s as

$$\begin{cases} \mu_i = -R_i^{-1} (C_i H_i^{-1} g_i + Q_i^\top \lambda - D_i), \\ Y_i^+ = Y_i^- - H_i^{-1} (g_i + C_i^\top \mu_i + A_i^\top \lambda). \end{cases} \quad (28)$$

V. NUMERICAL EXPERIMENT

In this section, we apply the three proposed algorithms to a practical MHE problem, known as the differential drive robots problem (see [14]). The following MHE problem involves three state variables, $x = (\phi, \psi, \theta)^\top$, which represent the lateral position ϕ , longitudinal position ψ , and orientation angle θ . Additionally, two control inputs, $u = (v, \omega)^\top$, are considered, where v denotes the linear velocity and ω the angular velocity. The observation vector $y = (r, \alpha)^\top$ consists of the relative range r and bearing α . Given x, u, y and a sampling time of $T = 0.2s$, the dynamics of the MHE system and the observer model are formulated as follows, in contrast to Equation (1):

$$f(x_n, u_n) = \begin{bmatrix} \phi_n \\ \psi_n \\ \theta_n \end{bmatrix} + T \begin{bmatrix} v_n \cos \theta_n \\ v_n \sin \theta_n \\ \omega_n \end{bmatrix}, y_n = \begin{bmatrix} r \\ \alpha \end{bmatrix} = \begin{bmatrix} \sqrt{\phi_n^2 + \psi_n^2} \\ \arctan(\frac{\psi_n}{\phi_n}) \end{bmatrix} + \begin{bmatrix} \nu_r \\ \nu_\alpha \end{bmatrix},$$

where ν_r and ν_α denote Gaussian noise, with $\nu_r \sim \mathcal{N}(0, \sigma_r^2)$ and $\nu_\alpha \sim \mathcal{N}(0, \sigma_\alpha^2)$.

The code implementation in this paper is based on [14]. The experimental setup adopts a prediction horizon $L = 25$, and the initial states $x_0 = (0.1, 0.1, 0.0)^\top$ define the initial position and orientation of the robot. In the implementation, the state trajectories $x^* = (\phi^*, \psi^*, \theta^*)^\top$ are generated via MPC under the same control model. Notably, the primal variables are initialized to $(\phi^*, \psi^*, 0)^\top$. In the numerical implementation of Algorithms 1 and 3, the penalty parameter is set to $\rho = 10^3$, while for Algorithm 2, $\rho = 25$. The dual variables λ and μ are initialized to zero. All simulations were conducted using Casadi-3.6.6 [1] with IPOPT in MATLAB R2024a on a Windows 11 system, equipped with a 2.1 GHz AMD Ryzen 5 4600U processor and 16GB of RAM.

Figure 2 compares the state trajectories obtained from centralized and distributed solvers for the MHE problem with $N = 4$. The results indicate that the proposed distributed MHE framework generates estimates nearly identical to those of the centralized baseline.

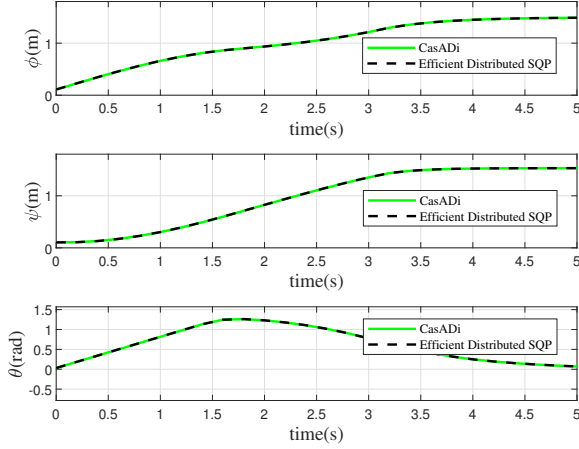


Fig. 2: Comparison of state estimation trajectories: Centralized Solver (CasADi) vs. Efficient Distributed SQP.

Figure 3 illustrates the convergence behavior of Algorithm 1–3 with $N = 4$, all exhibiting linear convergence. Notably, all three algorithms achieve an accuracy of 10^{-8} within 30 iterations, highlighting their computational efficiency. In particular, Algorithm 2 leverages CasADi to compute the exact solution in its first iteration, following the recommendations in [12, Algorithm 1].

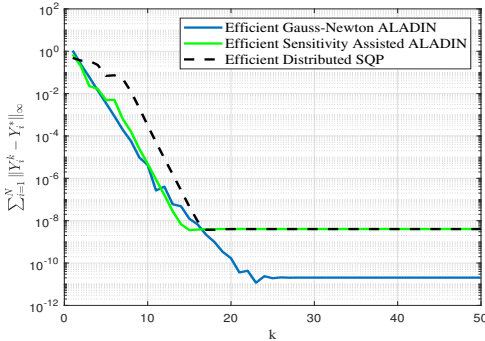


Fig. 3: Numerical convergence comparison among Algorithm 1-3

Table 1 summarizes the total CPU time of the three proposed efficient ALADIN variants as a function of the number of sub-windows N . Notably, existing time-splitting-based MPC studies lack theoretical analysis on the relationship between the number of sub-windows N and computational time. By leveraging Equations (11) and (13), we establish that the optimal number of sub-windows follows the asymptotic relation $N^* \approx \sqrt{L}$, where L denotes the total horizon length. For brevity, the detailed derivation will be provided in an extended version of this work. In our experiment, setting $L = 25$ yields an optimal sub-window count of $N^* = 5$. For comparison, we introduce **QP-CasADi**, which replaces Steps 2) and 3) of Algorithm 3 with CasADi-based QP solvers. The results demonstrate that across all

N	Algorithm 1	Algorithm 2	Algorithm 3	QP-CasADi
3	2.83	8.51	0.0183	1.60
4	2.84	8.76	0.0184	1.71
5	2.04	8.08	0.0155	1.57
6	3.05	11.82	0.0186	1.66

Table 1: Total CPU time [s] for different algorithms over N sub-windows (measured as the time for 50 iterations of each algorithm).

four algorithmic structures, the configuration with $N = 5$ consistently achieves the lowest computational time. Notably, although Algorithm 2 requires a longer total CPU time than Algorithm 1, its sub-problems solutions does not rely on existing solvers, making it particularly suitable for scenarios with limited computational resources at sub-nodes.

VI. CONCLUSION

This paper presents three computationally efficient distributed optimization algorithms for nonlinear MHE problems, accounting for the computational capabilities of sub-problem solvers. We first propose a distributed MHE reformulation based on a time-splitting strategy. Then, we develop novel solutions within the ALADIN algorithmic family. By leveraging the closed-form solution of large-scale coupled QP derived herein, these algorithms significantly reduce computational time, thus enabling real-time applications. Numerical experiments on an MHE problem including differential drive robots confirm the effectiveness of our algorithms, demonstrating superior convergence and computational efficiency. Future work will focus on enhancing the efficiency of the ALADIN framework by accelerating matrix updates in Algorithm 2 and adaptively prioritizing critical sub-problems during each iteration. Additionally, we will investigate the applicability of the proposed algorithms in broader practical scenarios.

APPENDIX I PROOF OF THEOREM 1

The augmented Lagrangian function for Problem (10) is defined as:

$$\begin{aligned} \mathcal{L}(\Delta X_i, \mu_i, \lambda) = & \sum_{i=1}^N \left(\frac{1}{2} \Delta X_i^\top H_i \Delta X_i + g_i^\top \Delta X_i \right) \\ & + \sum_{i=1}^N \mu_i^\top C_i \Delta X_i + \lambda^\top \sum_{i=1}^N A_i (X_i^+ + \Delta X_i). \end{aligned} \quad (29)$$

From (29), the KKT system of Problem (10) is given by:

$$\begin{cases} \frac{\partial \mathcal{L}}{\partial \Delta X_i} = H_i \Delta X_i + g_i + C_i^\top \mu_i + A_i^\top \lambda = 0, \\ \frac{\partial \mathcal{L}}{\partial \mu_i} = C_i \Delta X_i = 0, \\ \frac{\partial \mathcal{L}}{\partial \lambda} = \sum_{i=1}^N A_i (\Delta X_i + X_i^+) = 0. \end{cases} \quad (30)$$

From the first condition $\frac{\partial \mathcal{L}}{\partial \Delta X_i} = 0$ in Equation (30), the following expression is derived:

$$\Delta X_i = -H_i^{-1} (g_i + C_i^\top \mu_i + A_i^\top \lambda). \quad (31)$$

When Equation (31) is substituted into the second equation of (30), the resulting equation is expressed as:

$$\mu_i = -R_i^{-1} (C_i H_i^{-1} g_i + Q_i^\top \lambda). \quad (32)$$

Next, by substituting (32) into (31) and the third equation of (30), the following result is derived:

$$\sum_{i=1}^N G_i \lambda = p + \sum_{i=1}^N Q_i R_i^{-1} Q_i^\top \lambda.$$

Through further simplification, the solution for λ is obtained as Equation (19). Subsequently, the local dual variable μ_i is computed by Equation (32) using the previously computed λ . Finally, the local primal variable increment ΔX_i is calculated using Equation (31) based on the obtained μ_i and λ . Consequently, Problem (10) has been successfully solved.

APPENDIX II

DERIVATION OF SENSITIVITY INFORMATION

In this appendix, we detail the derivation of \mathcal{M}_i and \mathcal{N}_i . The augmented Lagrangian of Problem (9) is given by Equation (21). The KKT conditions associated with the constrained sub-problems are presented in Equation (22), as follows:

$$\varphi_i(\xi_i) = \begin{bmatrix} \nabla_{X_i}(J_i(X_i) + \mathcal{F}_i(X_i)^\top \mu_i) + A_i^\top \lambda + \rho(X_i - Y_i) \\ \mathcal{F}_i(X_i) \end{bmatrix}.$$

The solution manifold is further linearized, yielding the following equation:

$$s_i^+(\xi_i) = s_i(\xi_i^-) + \frac{\partial s_i}{\partial \xi_i}(\xi_i - \xi_i^-) + \mathcal{O}(\|\xi_i - \xi_i^-\|^2).$$

Given that $s_i(\xi_i^-)$ satisfies Equation (22), we apply the implicit function theorem, obtaining: $\frac{\partial \varphi_i}{\partial \xi_i}(s_i(\xi_i^-), \xi_i^-) = 0$, where $\frac{\partial \varphi_i}{\partial \xi_i}(s_i(\xi_i^-), \xi_i^-) = \frac{\partial \varphi_i}{\partial s_i} \frac{\partial s_i}{\partial \xi_i} + \frac{\partial \varphi_i}{\partial \xi_i}$. Furthermore,

$$\begin{cases} \frac{\partial \varphi_i}{\partial s_i} = \begin{bmatrix} \nabla_{X_i}^2 J_i + \rho I + \nabla_{X_i}^2 \mathcal{F}_i \mu_i & \nabla_{X_i} \mathcal{F}_i^\top \\ \nabla_{X_i} \mathcal{F}_i & \mathbf{0}_{|\mu_i| \times |\mu_i|} \end{bmatrix}, \\ \frac{\partial \varphi_i}{\partial \xi_i} = \begin{bmatrix} -\rho I & A_i^\top \\ \mathbf{0}_{|\mu_i| \times |Y_i|} & \mathbf{0}_{|\mu_i| \times |\lambda|} \end{bmatrix}. \end{cases} \quad (33)$$

In the end, we define: $\mathcal{M}_i = \frac{\partial \varphi_i}{\partial s_i}$, $\mathcal{N}_i = \frac{\partial \varphi_i}{\partial \xi_i}$. Thus, \mathcal{M}_i and \mathcal{N}_i in Equation (23) are obtained based on Equation (33).

REFERENCES

- [1] J. A. E. Andersson, J. Gillis, G. Horn, J. B. Rawlings, and M. Diehl. CasADi: a software framework for nonlinear optimization and optimal control. *Mathematical Programming Computation*, 11(1):1–36, Mar 2019.
- [2] K. Baumgärtner, R. Reiter, and M. Diehl. Moving horizon estimation with adaptive regularization for ill-posed state and parameter estimation problems. In *2022 IEEE 61st Conference on Decision and Control (CDC)*, pages 2165–2171, 2022.
- [3] S. Boyd, N. Parikh, E. Chu, B. Peleato, and J. Eckstein. Distributed optimization and statistical learning via the alternating direction method of multipliers. *Found. Trends Mach. Learn.*, 3(1):1–122, 2011.
- [4] M. Diehl, H. J. Ferreau, and N. Haverbeke. Efficient numerical methods for nonlinear mpc and moving horizon estimation. *Nonlinear model predictive control: towards new challenging applications*, pages 391–417, 2009.
- [5] X. Du, A. Engelmam, Y. Jiang, T. Faulwasser, and B. Houska. Distributed state estimation for AC power systems using Gauss-Newton ALADIN. In *In Proceedings of the 58th IEEE Conference on Decision and Control*, pages 1919–1924, 2019.
- [6] X. Du and J. Wang. Distributed consensus optimization with consensus ALADIN. In *American Control Conference*, 2025 (accepted for publication).
- [7] X. Du, J. Wang, X. Zhou, and Y. Mao. A bi-level globalization strategy for non-convex consensus ADMM and ALADIN, 2023.
- [8] B. Houska, J. Frasch, and M. Diehl. An augmented lagrangian based algorithm for distributed nonconvex optimization. *SIAM Journal on Optimization*, 26(2):1101–1127, 2016.
- [9] B. Houska and Y. Jiang. chapter Distributed Optimization and Control with ALADIN, pages 135–163. Springer, 2021.
- [10] Y. Jiang, C. N. Jones, and B. Houska. A time splitting based real-time iteration scheme for nonlinear mpc. In *2019 IEEE 58th Conference on Decision and Control (CDC)*, pages 2350–2355, 2019.
- [11] D. Kouzoupis, R. Quirynen, B. Houska, and M. Diehl. A block based ALADIN scheme for highly parallelizable direct optimal control. In *Proc. American Control Conf. (ACC)*, pages 1124–1129, July 2016.
- [12] D. Krishnamoorthy and V. Kungurtsev. A sensitivity assisted alternating directions method of multipliers for distributed optimization. In *2022 IEEE 61st Conference on Decision and Control (CDC)*, pages 295–300, 2022.
- [13] Z. Lin, H. Li, and C. Fang. *Alternating direction method of multipliers for machine learning*. Springer, 2022.
- [14] M. G. Mehrez. Mpc and mhe implementation in matlab using casadi. *github*, 2022.
- [15] J. Nocedal and S. Wright. *Numerical optimization*. Springer Science & Business Media, New York, 2006.
- [16] J. Püttschneider, J. Golembiewski, N. A. Wagner, C. Wietfeld, and T. Faulwasser. Towards event-triggered nmpc for efficient 6g communications: Experimental results and open problems. *arXiv preprint arXiv:2409.18589*, 2024.
- [17] J. B. Rawlings, D. Q. Mayne, M. Diehl, et al. *Model predictive control: theory, computation, and design*, volume 2. Nob Hill Publishing Madison, WI, 2017.
- [18] J. Shi, Y. Jiang, J. Oravec, and B. Houska. Parallel mpc for linear systems with state and input constraints, 2022.
- [19] L. Simpson, J. Asprion, S. Muntwiler, J. Köhler, and M. Diehl. Parallelizable parametric nonlinear system identification via tuning of a moving horizon state estimator, 2024.
- [20] G. Stomberg, A. Engelmam, M. Diehl, and T. Faulwasser. Decentralized real-time iterations for distributed nonlinear model predictive control. *arXiv preprint arXiv:2401.14898*, 2024.
- [21] G. Stomberg, A. Engelmam, and T. Faulwasser. Decentralized non-convex optimization via bi-level SQP and ADMM. In *2022 IEEE 61st Conference on Decision and Control (CDC)*, pages 273–278. IEEE, 2022.
- [22] G. Stomberg, M. Raetsch, A. Engelmam, and T. Faulwasser. Large problems are not necessarily hard: A case study on distributed nmpc paying off. *arXiv preprint arXiv:2411.05627*, 2024.
- [23] B. Wang, Z. Ma, S. Lai, and L. Zhao. Neural moving horizon estimation for robust flight control. *IEEE Transactions on Robotics*, 40:639–659, 2023.
- [24] A. Wynn, M. Vukov, and M. Diehl. Convergence guarantees for moving horizon estimation based on the real-time iteration scheme. *IEEE Transactions on Automatic Control*, 59(8):2215–2221, 2014.
- [25] L. Zou, Z. Wang, B. Shen, and H. Dong. Moving horizon estimation over relay channels: Dealing with packet losses. *Automatica*, 155:111079, 2023.